Current Molecular Biology Reports (2018) 4:25–33
https://doi.org/10.1007/s40610-018-0092-z

MOLECULAR BIOLOGY OF BONE MARROW FAT ADIPOSITY (B VAN DER EERDEN, SECTION EDITOR)

Molecular In Vivo Imaging of Bone Marrow Adipose Tissue

Stefan Ruschke[1] · Maximilian N. Diefenbach[1] · Daniela Franz[1] · Thomas Baum[2] · Dimitrios C. Karampinos[1]

Published online: 28 March 2018

Abstract

Purpose of Review The in vivo study of molecular processes in human bone marrow is important for both diagnostics and understanding of disease pathophysiology. Traditionally, the hematopoietic component of the bone marrow has been a research focus, but recently, the role of bone marrow adipose tissue has been gaining interest in many applications. The purpose of the present review is to give an overview of existing imaging modalities allowing in vivo molecular imaging of bone marrow adipose tissue in humans with an emphasis on technical aspects: the characteristics of the extracted parameters and their application in bone marrow adipose tissue.

Recent Findings Magnetic resonance (MR) imaging (MRI) and spectroscopy (MRS) are the most frequently used imaging methods for the examination of bone marrow adipose tissue as they provide rich soft tissue contrast and come without ionizing radiation. Existing MR methods allow the extraction of many different measures including proton density fat fraction, fatty acid characteristics, and diffusion and perfusion properties. However, many available techniques have to be carefully adjusted to be used in the investigation of the fat signal component, especially in the presence of trabecular bone. Dual-energy computed tomography (DECT) is an emerging technique—not yet widely available—which appears to be a promising alternative to MR for rapid fat fraction assessment. Positron emission tomography (PET) allows additional functional metabolic imaging and therefore provides valuable additional information (e.g., glucose uptake) to MR-based parameters at the cost of ionizing radiation.

Summary Bone marrow imaging still appears to be a niche with remaining technical challenges using existing imaging modalities. A good working knowledge of the underlying physical and technical principles is required as most techniques are yet not available out of the box and may need to be adjusted to fit the requirements for bone marrow adipose tissue imaging. In summary, MR, DECT, and PET enable the measurement of several inherently different parameters in in vivo molecular imaging of bone marrow adipose tissue. The growing interest for molecular imaging markers of bone marrow, thanks to its high metabolic and clinical significance, may eventually lead to new developments, as well as improvements of emerging techniques as soon as they become more broadly available.

Keywords Molecular imaging · Bone marrow adipose tissue · Bone marrow fat · Bone marrow adipocytes · Magnetic resonance imaging · Magnetic resonance spectroscopy

Introduction

Bone marrow describes one of the interior tissues of bones. Bone marrow is surrounded by cortical bone and comprises the hematopoietic component and the marrow adipose tissue (MAT). Depending on the type of bone, a trabecular bone network may be additionally present; if trabecular bone is present, the bone marrow fills up the cavities between the trabeculae. Traditionally, two main bone marrow compartments are differentiated based on their histological appearance: red and yellow bone marrow. Yellow bone marrow consists predominately of adipocytes, while red bone marrow

This article is part of the Topical Collection on *Molecular Biology of Bone Marrow Fat Adiposity*

✉ Stefan Ruschke
stefan.ruschke@tum.de

[1] Department of Diagnostic and Interventional Radiology, Klinikum rechts der Isar, Technical University of Munich, Ismaninger Str. 22, 81675 Munich, Germany

[2] Department of Diagnostic and Interventional Neuroradiology, Klinikum rechts der Isar, Technical University of Munich, Ismaninger Str. 22, Munich 81675, Germany

includes mainly hematopoietic cells but also some adipocytes. During the process of aging, red bone marrow is gradually converted to yellow bone marrow as a function of the skeletal site. In adults, the red bone marrow is mainly found in the axial skeleton. Recent findings have suggested to adjust the traditional concept of red and yellow bone marrow by a further MAT classification into constitutive and regulated MAT (cMAT/rMAT) [1, 2]. Specifically, Scheller et al. [3] introduced the concept of rMAT referring to bone marrow adipocytes interspersed with active hematopoiesis and its counterpart, cMAT which refers to bone marrow adipocytes in regions with low hematopoiesis and preservation upon systemic challenges.

In vivo molecular imaging of bone marrow adipose tissue is aiming at the spatially resolved characterization of its molecular content and the monitoring of molecular processes in the living organism. Suitable imaging modalities therefore require to interfere only insignificantly with the tissue and processes under investigation. Imaging modalities meeting the aforementioned requirements typically include magnetic resonance imaging (MRI), computed tomography (CT), and positron emission tomography (PET).

In the past, the hematopoietic component in bone marrow was the focus of most carried out research activities due to its obvious important role in disease such as leukemia or sickle-cell disease. However, for the last 10 years, there has been a growing interest also in the role of the adipose tissue residing in bone marrow and potential value of bone MAT (BMAT)-derived biomarkers [4–8], highlighted also by the formation of a new scientific society entirely focusing on bone marrow adipose tissue [9, 10].

The purpose of the present review is to provide an overview of (i) existing in vivo imaging modalities and (ii) their recent application in BMAT with an emphasis on research carried out in humans focusing on normal physiology in the last 5 years. Therefore, technical aspects are presented in the first part of the review, while the second part then describes their application in recent studies.

Literature Search

A literature search was conducted using the electronic PubMed database (http://www.ncbi.nlm.nih.gov/pubmed) in December 2017 in order to identify relevant publications of the last 5 years. Search terms used included the term "bone marrow adipose tissue / adipocytes / fat" and one or more of the following terms: "imaging, spectroscopy, MRI, PET, CT." General inclusion criteria included publication in English and in vivo studies in humans with respect to normal physiology, and MR-based methods were required to be at least semi-quantitative. Exceptions to the inclusion criteria of "*in vivo* studies in humans with respect to normal physiology" were made if only very limited literature was available on a particular topic or to emphasize on technical or translational aspects. The references of relevant articles were also screened.

Technical Aspects of Bone Marrow Adipose Tissue Imaging

A variety of histological and optical imaging modalities investigating different chemical and physical properties exist that can theoretically be used to examine BMAT. However, most of such histological and optical imaging modalities that may be used to examine BMAT are implicitly invasive to a certain extent, e.g., as they require biopsy. Magnetic resonance (MR), CT, and PET are the three most commonly used modalities in in vivo non-invasive characterization of human BMAT. Compared to histology, in vivo imaging modality techniques have much lower spatial resolution, but allow the examination of tissue within the living organism and can easily cover much larger anatomical regions. The technical aspects of using MR, CT, and PET for in vivo imaging of human BMAT are briefly discussed in the following.

Magnetic Resonance

MR is particularly suitable for the characterization of BMAT thanks to its manifold and high soft tissue contrast. The fact that MR is a non-ionizing technique makes it furthermore very attractive in cross-sectional or longitudinal studies involving humans where ionizing radiation and invasive procedures are a safety and ethical concern. However, one disadvantage is the longer scan time and higher cost of MR as compared to CT. Conventional MRI usually involves only the assessment of qualitative contrasts (e.g., T1-weighted and T2-weighted images) which are used to identify qualitative abnormal signal patterns with application, e.g., in the diagnosis of bone marrow lesions and treatment monitoring of pathologies including bone marrow malignancies, bone metastases, and multiple myeloma [11]. The extraction of quantitative parameters using MR requires additional effort as this involves the often non-trivial elimination of confounding effects. Over the last years, increasingly more quantitative MR techniques have been emerging allowing to investigate molecular properties including diffusion properties [12], cellularity [13], proportional water–fat content [14], and fatty acid characterization [15]. The application of quantitative MR methods in bone marrow has also recently been reviewed by Karampinos et al. [16].

Bone marrow MR primarily focuses on the hydrogen proton properties of water and fat molecules within the bone marrow. Hydrogen protons experience a shielding effect originating from the surrounding electron clouds which depend on the embedding chemical structure. The difference in the

shielding effect leads to a different chemical shift which is an important property for differentiating water and fat molecules. MR spectroscopy (MRS) allows the extraction of rich information in the chemical shift domain but with only limited spatial information. This is particularly true for single-voxel MRS (SV-MRS) where the signal information is averaged over a volume of interest and therefore multiple measurements are required to gain information about spatial variation. In order to receive spatial information, MRI methods can be used, which in contrast to MRS only provide limited information in chemical shift domain. The combination of both MRS and MRI is referred to as MR spectroscopic imaging (MRSI) but is rarely found in musculoskeletal applications due to the extensively prolonged scan time and many technical challenges. Chemical shift encoding-based imaging (CSEI) tries to fill the gap between MRS and MRSI. CSEI is typically based on an imaging sequence that also acquires some additional information in the chemical shift domain maintaining reasonable scan times. The additional information in the chemical shift domain can then be used to model the parameters of interest. CSEI has been heavily used to differentiate between proton signals coming from water and fat molecules and is also known as *Dixon* imaging.

The most commonly used proton MR-based parameters in BMAT are briefly described in the following section and include fat fraction, metrics of fatty acid composition, diffusion, perfusion, and magnetization transfer.

Fat Fraction

Fat fraction measurements using MR refer to the definition of the fat fraction as the ratio of the MR-measured fat signal over the sum of the MR-measured fat plus water signal. Fat fraction is one of the most commonly investigated parameters in BMAT. Traditionally, fat fraction measurements have been dependent on the employed MR technique as well as the selected MR sequence parameters and should therefore only be considered as semi-quantitative and are referred to as signal-weighted fat fraction (sFF) from here on. More recent efforts have been aiming at removing confounding factors (e.g., relaxation time weighting) in order to achieve a quantitative fat fraction measure reflecting the proton density ratio of water and fat also known as proton density fat fraction (PDFF) [17].

MRS achieves high reproducibility in the measurement of fat fraction and is therefore usually considered as the MR gold standard for fat fraction measurements. This has been shown for sFF measurements using SV-MRS in femoral bone marrow [18] and also vertebral bone marrow [19, 20].

The extraction of PDFF values using SV-MRS methods also requires the consideration of confounding factors. As shown by Dieckmeyer et al. [21•], the correction of T2 relaxation is not only required to obtain correct PDFF measurements but also showed a strong effect on the obtained fat fraction values arising from the negative correlation of the T2 of water with age in female subjects.

Bone marrow fat fraction measurements have also been validated against histology by MacEwan et al. [13] and Arentsen et al. [22] yielding good inter-modality correlation of vertebral bone marrow fat fraction values with histology.

CSEI-based water–fat imaging has been shown to achieve high accuracy and reproducibility in the assessment of PDFF [23]. Furthermore, it enables spatially resolved fat fraction mapping in a reasonable acquisition time, which is, e.g., beneficial in whole spine imaging [24, 25•]. Nevertheless, in the assessment of BMAT PDFF, additional confounding factors have to be acknowledged, i.e., a fat fraction bias due to the presence of trabecular bone [26, 27] and T2* relaxation effects [28]. Figure 1 shows exemplary whole spine PDFF maps in two pediatric subjects.

Le Ster et al. [30, 31] investigated CSEI for measuring not only PDFF but also T1 and T2* of water and fat comparing the bone marrow of the lumbar spine, sternum, humerus, ilium, and femur. Using their technique, Le Ster et al. [31] reported a strong negative correlation between the T1 of water and PDFF.

Fatty Acid Characterization

Covalent bound protons in lipids experience a shielding effect depending on the surrounding electron clouds and therefore comprise information about the chemical structure in the direct neighborhood. The difference in the shielding effect leads to a different chemical shift which can then be measured using, e.g., MRS. Assuming that all signal rising protons belong to water and triacylglycerides (TAGs) only, a mixture of saturated, mono-unsaturated, and poly-unsaturated TAGs can be characterized by three main parameters: the number of double bonds per TAG (ndb), the number of methylene-interrupted double bonds per TAG (nmidb), and the mean fatty acid carbon chain length (CL) [32]. However, due to the limited linewidths that can be achieved and the dominant water signal in some bone marrow compartments (e.g., in the spine), it is sometimes only feasible to extract, e.g., a measure of unsaturation based on a measured peak ratio. To overcome issues with the dominant water peak in vertebral bone marrow, especially in younger subjects, long echo time measurements (stimulated echo acquisition mode (STEAM) with TE = 100 ms and TM = 20 ms or point resolved spectroscopy (PRESS) with TE = 200 ms) have been proposed for bone marrow unsaturation measurements albeit the decreased SNR and additional *J*-coupling modulation of the signal [33, 34]. Fallone et al. [35] reported recently that also the estimation of relative omega-3 fatty acid concentration is feasible in tibial bone marrow using optimized MRS parameters (STEAM with TE = 120 ms, TM = 20 ms, and PRESS with TE = 180 ms). Furthermore, the extracted parameters may also

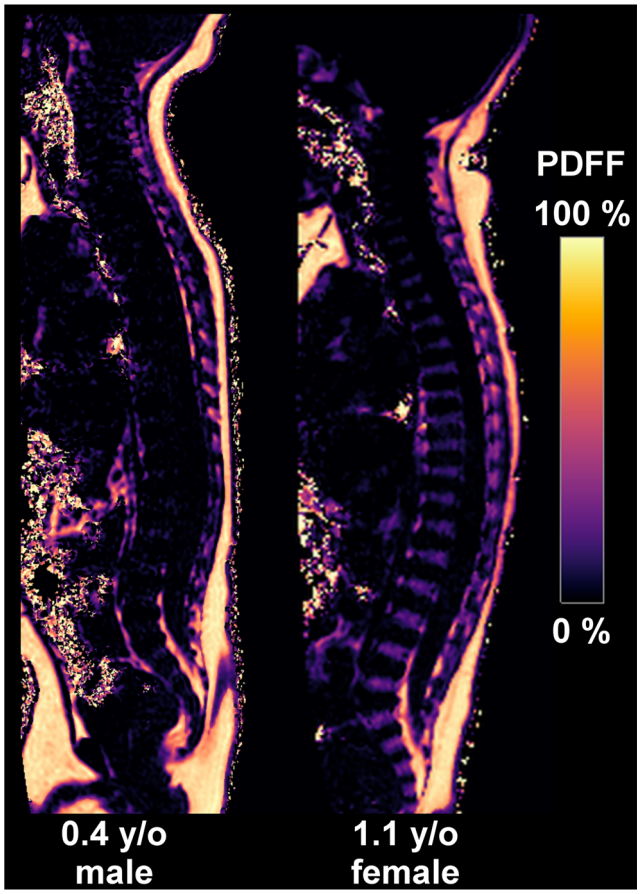

Fig. 1 Example PDFF maps from [29] using CSEI at 3 T. PDFF measurements in lumbar vertebral bone marrow yield values close to 0% and around 15% in the 0.4-y/o male and 1.1-y/o female, respectively. Courtesy of Houchun H. Hu and Jeffrey H. Miller from Phoenix Children's Hospital, AZ, USA. y/o, year-old

largely vary depending on the employed peak fitting method: in order to achieve reliable and reproducible parameter quantification, Xu et al. [36] recently proposed a combination of a frequency model and time-domain analysis. Yet, there is no consensus on the optimal quantification strategy for the extraction of bone marrow fatty acid characteristics.

Diffusion

Diffusion effects due to *Brownian* motion induce additional attenuation of the acquired signal. The extracted signal information can be associated with the bone marrow microstructure yielding information beyond the imaging resolution. Studies including quantitative diffusion measurements usually report an apparent diffusion coefficient (ADC) to also acknowledge remaining confounding effects such as restricted diffusion [37]. Diffusion measurements have been mainly focusing on the water component in BMAT where (residual) fat signal is usually considered as a confounding effect [38•]. Due to the low diffusion coefficient of lipids compared to the diffusion coefficient of water, the required *b* values for fat diffusion measurements (a measure reflecting the strength and timing of the diffusion-weighting gradients) increase, and therefore also the sensitivity to incoherent motion increases as well. Steidle et al. [39] employed diffusion-weighted (DW) echo-planar imaging (EPI) at 1.5 T with *b* values up to 50,000 s/mm^2 in the lower extremities and extracted ADC values in tibial BMAT in the order of 2×10^{-5} mm^2/s. For comparison, the ADC of water in vertebral bone marrow is two orders of magnitude higher [40].

Perfusion

Perfusion MRI allows the extraction of blood delivery-associated parameters including, e.g., blood volume and blood flow. Bone marrow perfusion measurements are commonly based on T1-weighted dynamic contrast-enhanced (DCE) MRI using either a semi-quantitative approach based on, e.g., the maximum enhancement or the slope of the signal–time curve or a quantitative approach which requires the arterial input function and kinetic analysis of the tracer [41]. Many studies have employed a semi-quantitative approach, although the presence of BMAT as a confounder may require a quantitative analysis [42].

Magnetization Transfer

Magnetization transfer (MT) describes the interaction between (usually) two proton pools with an inherent different T2-decay, e.g., a free proton pool with long T2 relaxation time and a bound proton pool (e.g., bound to macromolecules) with short T2 relaxation. MT in bone marrow using MRS was first investigated by Schick et al. [43] and then also picked up in other technical studies [44–46]. However, there were no recent research activities published with respect to this technique.

Computed Tomography

CT measures the attenuation characteristics of ionizing gamma rays penetrating the object of interest. The advantage of CT is its short acquisition time compared to MRI and PET. Conventional CT shows typically only a low soft tissue contrast which makes it difficult to monitor quantitative changes in bone marrow. In order to obtain a quantitative measure, CT images have to be calibrated—usually using a calibration phantom—in order to obtain the quantitative attenuation measure Hounsfield unit (HU). Newly emerging techniques including multi-energy CT (MECT) and dual-energy CT (DECT) allow the differentiation of elemental compositions enabling mass density quantification of a given material mixture with known elemental composition [47]. The additional degree of information using MECT [48] and DECT can not only improve bone mineral density measurements [49, 50] but

also help in the diagnosis of bone marrow lesions [51, 52] and DECT-based fat fraction measurements were found to be in agreement with single voxel MRS [22, 53•] and CSEI [54]. Recently, Arentsen et al. [55] presented a DECT-based method for MAT quantification including high correlation with sFF obtained with CSEI. Additionally, marrow-corrected volumetric bone mineral density measurements were obtained with potential application in the monitoring of bone health.

Positron Emission Tomography

PET is the classical imaging modality of choice for functional metabolic imaging. It is usually combined with CT or MRI to acquire also anatomical information on which the metabolic function can be mapped. The technique itself is based on the detection of paired gamma rays indirectly sent out by a positron-emitting (beta particle) radionuclide which is also called the tracer. This tracer is bound in a molecule which is biologically active in the metabolic process of interest. The most commonly used tracer is a glucose analog called fluorine-18 (F-18) fluorodeoxyglucose (FDG) due to its important role in oncology for the diagnosis of tumors and metastasis [56]. FDG is picked up by the glucose metabolism and is therefore indicating cell proliferation. One tracer that is particularly used in bone imaging is F-18-labeled NaF (^{18}F-fluoride) [57] due to its high and rapid bone uptake in combination with rapid blood clearance resulting in a high bone-to-background ratio. Other tracers which appear interesting in the context of BMAT are C-11-labeled methionine which is involved in the synthesis of phospholipids [58, 59] and copper-64-labeled liposomes, which showed good results selectively targeting bone marrow tumors in an animal study by Lee et al. [60].

Applications of Molecular Imaging in Recent Bone Marrow Adipose Tissue Studies

Molecular imaging of BMAT is gaining in attention as a perspective in clinical applications in osteoporosis, diabetes, anorexia nervosa, and obesity [6, 61, 62]. However, before an imaging method can be used in a clinical application, the technique has to be tested in terms of its accuracy, reproducibility, and robustness. The following section summarizes recent studies investigating normal BMAT physiology and selected studies that are of particular interest due to the applied methodology. An accompanying overview of main findings is given in Table 1.

Magnetic Resonance

Normal spinal bone marrow fat fraction development as a function of age using MR has been investigated in numerus studies. First studies by Kugel et al. [63] and Griffith et al. [64] investigated BMAT sFF in the L3 vertebra as a function of age using MRS. Griffith et al. reported based on their own data and data from Kugel et al. that sFF was higher in men compared to that in women in age groups from 11 to 60 years but then reversed in the age groups from 60 to 90 years because of stronger increase of sFF in women compared to men after menopause. This trend was also confirmed by several other studies [13, 65, 66, 71]. Ruschke et al. [29] reported 0% PDFF shortly after birth followed by a strong increase in PDFF as a function of age independent of sex employing CSEI in pediatrics. Intra-individual bone marrow fat fraction variations as function of vertebra location were first investigated using MRS [19] and showed increasing sFF from the L1 to L4 vertebral bodies. Using CSEI-based PDFF measurement, this trend could be confirmed from C3 to L5 [25•, 29] with an absolute precision error of 1.7% [25•] averaged over the whole spine. Mistry et al. [70] found in a Reykjavik cohort that higher bone marrow fat fraction assessed in the lumbar spine is also associated with lower total testosterone and estradiol levels in older men. A similar trend was also non-significantly observed in older females.

In 2013, Patch et al. [75] reported in a study that a decrease in unsaturation levels and an increase in saturation levels in vertebral bone marrow fat were both associated with a higher prevalence of fragility fractures even after adjustment for age and BMD in diabetic patients. Interestingly, fat fraction did not show any correlation with fracture status. Consequently, this finding raised interest in the assessment of fatty acid characteristics of bone marrow. Fatty acid unsaturation was also characterized in the L3 vertebra as a function of age by Maciel et al. [66]. Maciel et al. reported that increasing BMAT fat fraction and saturated lipid level are correlating with age. Li et al. [68] investigated similar parameters in the iliac crest using ex vivo proton MAS NMR and reported lowered lipid unsaturation and elevated lipid saturation levels with decreasing bone mineral density. Histomorphometry of transiliac crest biopsy also correlated with sFF determined in the L3 vertebra whereas there was no association with femoral sFF [69]. Pansini et al. [67] compared sFF measurements at different bone marrow sites and reported an age- and sex-independent fat fraction gradient decreasing from the greater trochanter to the femoral head to the femoral neck to the diaphysis and finally to the acetabulum. The trend of an increasing bone marrow fat fraction was also found in the ilium and intertrochanteric femur from premenopausal to postmenopausal women while the assessed PDFF in the great trochanter was not correlating with age [72].

Diffusion characteristics of bone marrow were predominantly examined in the spine for the differentiation of benign and malignant vertebral compression fractures. However, the extracted absolute ADC values rely on the applied method and range between 0.2 and 0.6×10^3 mm^2/s in normal vertebral bone marrow making it difficult to compare different studies [40].

Bone marrow perfusion characteristics were investigated in osteoporotic patients with acute vertebral fractures by Biffar

Table 1 Summary of selected studies recently investigating bone marrow adipose tissue reporting parameters associated with normal physiology

Modality	Effect/main observation	Cohort	Measurement details	Study
MRS	Spine L3: sFF ↑ with age; sFF in men > sFF in women for all age groups from 11 to 60+ years	154 ♀ + ♂	sFF with SV-PRESS (TR/TE = 2000/40 ms) @ 1.5 T	[63]
	Spine L3: sFF ↑ with age; sFF in men > sFF in women for all age groups from 11 to < 60 years; sFF in men < sFF in women for all age groups from 60 to 90 years	145 ♀, 114 ♂	sFF with SV-PRESS (TR/TE = 3000/25 ms) @ 1.5 T	[64]
	sFF ↑ in spine from L1 to L4	51 ♀	sFF with SV-PRESS (TR/TE = 3000/37 ms) @1.5 T	[19]
	Spine L1 to L5: sFF ↑ with age; sFF in men > sFF in women for age groups from 30 to 39 years; sFF in men ~ = sFF in women for age groups from 40 to 69 years	24 ♀, 20 ♂	sFF with SV-PRESS (TR/TE = 1500/30 ms) @ 3 T	[65]
	Spine L3: FF ↑, saturation ↑, unsaturation ↑ with age	30 ♀, 21 ♂	FF with SV-PRESS (TR = 2000 ms TE = 40/60/80 ms) @ 3 T	[66]
	Acetabulum, femoral head, femoral neck, greater trochanter, and diaphysis: sFF from high to low (age and sex independent): greater trochanter > femoral head > femoral neck > diaphysis > acetabulum	40 ♀, 40 ♂	sFF with SV-STEAM (TR/TE = 5000/20 ms) @ 3 T	[67]
	Iliac crest: ↓ unsaturation and ↑saturation levels with ↓ BMD	24 ♀	MAS NMR: in vitro (iliac crest aspiration)	[68]
	Spine L3 and femur: transiliac crest biopsies correlates with sFF in L3 vertebrae but not with proximal femur	16 ♀	sFF with SV-PRESS (TR/TE = 3000/25 ms) @ 1.5 T	[69]
	Spine L1 to L4: sFF ↑ is associated with ↓ total estradiol and testosterone levels in older men; same non-significant association also in older women	226 ♀, 244 ♂	sFF with SV-PRESS @ 1.5 T	[70]
MRI	Spine L4 or L5: sFF ↑ with age faster for women compared to men	44 ♀ + ♂	sFF with 2-echo-CSEI @ 3 T	[71]
	Lumbar spine, ilium, and intertrochanteric femur: PDFF ↑ with age; average PDFF of post- menopausal females > pre-menopausal females; greater trochanter: PDFF no correlation with age	31 ♀	PDFF with 6-echo-CSEI @ 3 T	[72]
	Spine C3 to L5: mean PDFF ↑ from C3 to L5; absolute precision error of 1.7% averaged over C3 to L5;	11 ♀, 17 ♂	PDFF with 8-echo-CSEI @ 3 T	[25]
	Spine C3 to L5: mean PDFF ↑ from C3 to L5; PDFF correlates natural logarithm of age	49 ♀, 44 ♂	PDFF with 6-echo-CSEI @ 3 T	[29]
	Normal vertebral bone marrow ADC between 0.2 and 0.6×10^3 mm^2/s		Meta-analysis of 16 studies @ 1-3 T	[40]
	Spine T8 to L5: mean plasma flow and volume ↓ from T8 to L5;	6 ♀, 4 ♂	DCE-MRI @ 1.5 T	[42]
DECT	Spine C3 to L5: ↑ fat fraction from C3 to L5	20 ♀; 24 h PM	DECT: 80 kVp/140 kVp	[55]
PET	Higher red bone marrow volume per body weight in men compared to women; red/yellow bone marrow ratio in the intraosseous volume in women > men	102 ♀ + ♂; patients	FDG-PET/CT	[73]
	Humerus, T-spine, L-spine, pelvis, femur: ↓ sFF with ↑ SUV; ↓ sFF with ↑ ADC	110 ♀ + ♂; patients	FDG-PET/MRI; MRI: 2-echo-CSEI, ssDW-EPI @ 3 T	[74••]

♀, women; ♂, men; *kVp*, peak kilovoltage; *PM*, postmortem; *ss*, single -shot

et al. [42]. In their control group (10 subjects), Biffar et al. reported decreasing quantitative plasma flow and plasma volume from the T8 to L5 vertebrae. In a quantitative DCE-MRI study by Breault et al. [76], the two groups of women with age under and over 50 years, respectively, showed only slight effects of age and on perfusion parameters.

Computed Tomography

There is very limited data available exploring normal physiology of BMAT in vivo using DECT-based methods. Recently, Arentsen et al. [55] assessed DECT-based BMAT fat fractions (DECT-FF) using full body DECT in women within 24 h postmortem. They showed a high correlation of DECT-based fat fraction with sFF using CSEI. In agreement with other MRI-based studies [25•, 29], they also reported increasing fat fraction from C3 to L5 vertebra using their method.

Positron Emission Tomography

FDG-PET/CT was employed by Sambuceti et al. [73] to examine bone marrow extension and activity throughout the whole body in non-metastatic melanoma patients. The CT

images allowed Sambuceti et al. to precisely define the intraosseous volume which could then be used to mask bone marrow in the FDG-standardized uptake values (SUV) maps. Subsequently, for mean spine SUV − 2.5 times the measured standard deviation was defined as red marrow, while voxels with SUV < 1.11 were defined as yellow marrow. As a result, they found a higher prevalence of red bone marrow in the axial skeleton and higher red bone marrow volume per body weight in men compared to women. However, the red/yellow bone marrow ratio in the intraosseous volume was higher in women compared to that in men. Although not statistically assessed, red/yellow bone marrow ratio tended to slightly decrease from cervical to lumbar spine. Furthermore, the age showed an inverse correlation with the extracted red bone marrow volume while this trend was less pronounced in average red bone marrow SUV.

Schraml et al. [74••] analyzed bone marrow fat fraction, ADC, and metabolic activity measured as SUV in various skeletal sites in 110 cancer patients using 18F-FDG-PET/MR. MRI included sFF using CSEI and diffusion-weighted echo-planar imaging. They found an inverse correlation between sFF and SUV, as well as sFF and ADC, respectively. Increasing mean sFF (from low to high) was measured in T-spine, L-spine, pelvis, femur, and humerus with respective inverse correlations of SUV and ADC excepting for the T-spine which correction between sFF and ADC did not reach significance.

FDG-PET is also considered as the imaging gold standard for brown adipose tissue quantification. FDG-PET measurements investigating brown adipose tissue also show an uptake in the bone marrow, especially in the spinal bone marrow, which among other findings [77] suggest potential similarities. For example, Lee et al. [78] investigated the relationship between brown adipogenesis and bone mineral density using FDG-PET and found that higher BMD was associated with brown adipose tissue volume in women, while there was no correlation in men. Unfortunately, this study did not include further characterization of the bone marrow uptake and its potential relation with BMD.

Conclusions

Available techniques for in vivo metabolic imaging of BMAT are not widespread and require a good understanding of the underlying technical and physical principles. Currently, the most commonly used modalities include MR, CT, and PET, whereas MR holds the biggest share due to its non-invasive and non-ionizing properties. MR allows the measurement of many different parameters that may be of interest in BMAT including fat fraction, fatty acid characteristics, diffusion, perfusion, and magnetization transfer. However, many available techniques—except for fat fraction assessment and fatty acid characterization—have been developed and extensively tested for water proton signals and can therefore not directly be applied to the spectrally more complex fat signal. Conventional CT itself is not applicable to measure BMAT properties but new developments towards DECT, which allow simple tissue decomposition, maybe used in the future when they come broadly available. PET, often combined with CT or MRI, allows to obtain information about a specific metabolic function based on the given tracer, e.g., FDG-PET can be used to label the glucose metabolism in BMAT. It is expected that additional effort will be put into technical developments for in vivo metabolic imaging of BMAT since BMAT has been gaining attention over the last years due to potential clinical applications in, e.g., osteoporosis, diabetes, and obesity.

Funding Information Thomas Baum received grant support from the Technical University of Munich, Faculty of Medicine (KKF H01). Dimitrios C. Karampinos received grant support from Philips Healthcare.

Compliance with Ethical Standards

All reported studies/experiments with human or animal subjects performed by the authors have been previously published and complied with all applicable ethical standards (including the Helsinki declaration and its amendments, institutional/national research committee standards, and international/national/institutional guidelines).

Conflict of Interest Stefan Ruschke, Maximilian N. Diefenbach, Daniela Franz, and Thomas Braum declare no conflicts of interest. Dimitrios C. Karampinos reports grants from Philips Healthcare, during the conduct of study and outside the submitted work.

Human and Animal Rights and Informed Consent This article does not contain any studies with human or animal subjects performed by any of the authors.

References

Papers of particular interest, published recently, have been highlighted as:
- • Of importance
- •• Of major importance

1. Scheller EL, Rosen CJ. What's the matter with MAT? Marrow adipose tissue, metabolism, and skeletal health. Ann N Y Acad Sci. 2014;1311:14–30.
2. Devlin MJ, Rosen CJ. The bone-fat interface: basic and clinical implications of marrow adiposity. Lancet Diabetes Endocrinol. 2015;3:141–7.
3. Scheller EL, Doucette CR, Learman BS, Cawthorn WP, Khandaker S, Schell B, et al. Region-specific variation in the properties of skeletal adipocytes reveals regulated and constitutive marrow adipose tissues. Nat Commun. 2015;6:7808.
4. Motyl KJ, Guntur AR, Carvalho AL, Rosen CJ. Energy metabolism of bone. Toxicol Pathol. 2017;45:887–93.
5. Horowitz MC, Berry R, Holtrup B, Sebo Z, Nelson T, Fretz JA, et al. Bone marrow adipocytes. Adipocyte. 2017;6:193–204.
6. Schwartz AV. Marrow fat and bone: review of clinical findings. Front Endocrinol. 2015;6:40.

7. Veldhuis-Vlug AG, Rosen CJ. Clinical implications of bone marrow adiposity. J Intern Med. 2017;283:121–39. https://doi.org/10.1111/joim.12718.
8. Zhou BO, Yu H, Yue R, Zhao Z, Rios JJ, Naveiras O, et al. Bone marrow adipocytes promote the regeneration of stem cells and haematopoiesis by secreting SCF. Nat Cell Biol. 2017;19:891–903.
9. Hardouin P, Marie PJ, Rosen CJ. New insights into bone marrow adipocytes: report from the first European meeting on bone marrow adiposity (BMA 2015). Bone. 2016;93:212–5.
10. van der Eerden B, van Wijnen A. Meeting report of the 2016 bone marrow adiposity meeting. Adipocyte. 2017;6:304–13.
11. Moulopoulos LA, Koutoulidis V. Bone marrow MRI: a pattern-based approach; 2015. p. 1–172.
12. Khoo MMY, Tyler PA, Saifuddin A, Padhani AR. Diffusion-weighted imaging (DWI) in musculoskeletal MRI: a critical review. Skelet Radiol. 2011;40:665–81.
13. MacEwan IJ, Glembotski NE, D'Lima D, Bae W, Masuda K, Rashidi HH, et al. Proton density water fraction as a biomarker of bone marrow cellularity: validation in ex vivo spine specimens. Magn Reson Imaging. 2014;32:1097–101.
14. Hu HH, Kan HE. Quantitative proton MR techniques for measuring fat. NMR Biomed. 2013;26:1609–29.
15. Berglund J, Ahlström H, Kullberg J. Model-based mapping of fat unsaturation and chain length by chemical shift imaging-phantom validation and in vivo feasibility. Magn Reson Med. 2012;68:1815–27.
16. Karampinos DC, Ruschke S, Dieckmeyer M, Diefenbach M, Franz D, Gersing AS, et al. Quantitative MRI and spectroscopy of bone marrow. J Magn Reson Imaging. 2017;7:448.
17. Reeder SB, Hu HH, Sirlin CB. Proton density fat-fraction: a standardized mr-based biomarker of tissue fat concentration. J Magn Reson Imaging. 2012;36:1011–4.
18. Pansini VM, Monnet A, Salleron J, Penel G, Migaud H, Cotten A. Reproducibility of 1H MR spectroscopy of hip bone marrow at 3 tesla. J Magn Reson Imaging. 2012;36:1445–9.
19. Li X, Kuo D, Schafer AL, Porzig A, Link TM, Black D, et al. Quantification of vertebral bone marrow fat content using 3 tesla MR spectroscopy: reproducibility, vertebral variation, and applications in osteoporosis. J Magn Reson Imaging. 2011;33:974–9.
20. Singhal V, Miller KK, Torriani M, Bredella MA. Short- and long-term reproducibility of marrow adipose tissue quantification by 1H-MR spectroscopy. Skelet Radiol. 2016;45:221–5.
21.• Dieckmeyer M, Ruschke S, Cordes C, Yap SP, Kooijman H, Hauner H, et al. The need for T_2 correction on MRS-based vertebral bone marrow fat quantification: implications for bone marrow fat fraction age dependence. NMR Biomed. 2015;28:432–9. **This study shows the confounding effect of T2 weighting on MRS measurements in vertebral bone marrow and why PDFF should be measured instead of sFF.**
22. Arentsen L, Yagi M, Takahashi Y, Bolan PJ, White M, Yee D, et al. Validation of marrow fat assessment using noninvasive imaging with histologic examination of human bone samples. Bone. 2015;72:118–22.
23. Hernando D, Sharma SD, Aliyari Ghasabeh M, et al. Multisite, multivendor validation of the accuracy and reproducibility of proton-density fat-fraction quantification at 1.5T and 3T using a fat-water phantom. Magn Reson Med. 2016; https://doi.org/10.1002/mrm.26228.
24. Martin J, Nicholson G, Cowin G, Ilente C, Wong W, Kennedy D. Rapid determination of vertebral fat fraction over a large range of vertebral bodies. J Med Imaging Radiat Oncol. 2014;58:155–63.
25.• Baum T, Yap SP, Dieckmeyer M, Ruschke S, Eggers H, Kooijman H, et al. Assessment of whole spine vertebral bone marrow fat using chemical shift-encoding based water-fat MRI. J Magn Reson Imaging. 2015;42:1018–23. **Study on whole spine quantitative PDFF mapping achieving an absolute precision error of 1.7%.**
26. Karampinos DC, Melkus G, Baum T, Bauer JS, Rummeny EJ, Krug R. Bone marrow fat quantification in the presence of trabecular bone: initial comparison between water-fat imaging and single-voxel MRS. Magn Reson Med. 2013;71:1158–65.
27. Gee CS, Nguyen JTK, Marquez CJ, et al. Validation of bone marrow fat quantification in the presence of trabecular bone using MRI. J Magn Reson Imaging. 2014;42:539–44.
28. Karampinos DC, Ruschke S, Dieckmeyer M, Eggers H, Kooijman H, Rummeny EJ, et al. Modeling of T2* decay in vertebral bone marrow fat quantification. NMR Biomed. 2015;28:1535–42.
29. Ruschke S, Pokorney A, Baum T, Eggers H, Miller JH, Hu HH, et al. Measurement of vertebral bone marrow proton density fat fraction in children using quantitative water-fat MRI. Magn Reson Mater Phys Biol Med. 2017;30:449–60.
30. Le Ster C, Gambarota G, Lasbleiz J, Guillin R, Decaux O, Saint Jalmes H. Breath-hold MR measurements of fat fraction, T1, and T2* of water and fat in vertebral bone marrow. J Magn Reson Imaging. 2016;44:549–55.
31. Le Ster C, Lasbleiz J, Kannengiesser S, Guillin R, Gambarota G, Saint Jalmes H. A fast method for the quantification of fat fraction and relaxation times: comparison of five sites of bone marrow. Magn Reson Imaging. 2017;39:157–61.
32. Hamilton G, Hamilton G, Yokoo T, et al. In vivo characterization of the liver fat ^{1}H MR spectrum. NMR Biomed. 2011;24:784–90.
33. Troitskaia A, Fallone BG, Yahya A. Long echo time proton magnetic resonance spectroscopy for estimating relative measures of lipid unsaturation at 3 T. J Magn Reson Imaging. 2013;37:944–9.
34. Bingölbali A, Fallone BG, Yahya A. Comparison of optimized long echo time STEAM and PRESS proton MR spectroscopy of lipid olefinic protons at 3 Tesla. J Magn Reson Imaging. 2015;41:481–6.
35. Fallone CJ, McKay RT, Yahya A. Long TE STEAM and PRESS for estimating fat olefinic/methyl ratios and relative ω-3 fat content at 3T. J Magn Reson Imaging. 2017;24:238.
36. Xu K, Sigurdsson S, Gudnason V, Hue T, Schwartz A, Li X. Reliable quantification of marrow fat content and unsaturation level using in vivo MR spectroscopy. Magn Reson Med. 2017;19:109.
37. Le Bihan D, Breton E, Lallemand D, Grenier P, Cabanis E, Laval-Jeantet M. MR imaging of intravoxel incoherent motions: application to diffusion and perfusion in neurologic disorders. Radiology. 1986;161:401–7.
38.• Dieckmeyer M, Ruschke S, Eggers H, Kooijman H, Rummeny EJ, Kirschke JS, et al. ADC quantification of the vertebral bone marrow water component: removing the confounding effect of residual fat. Magn Reson Med. 2016;46:601. **Study showing the confounding effect of the lipid signal in quantitative diffusion-weighted MRI.**
39. Steidle G, Eibofner F, Schick F. Quantitative diffusion imaging of adipose tissue in the human lower leg at 1.5 T. Magn Reson Med. 2011;65:1118–24.
40. Dietrich O, Geith T, Reiser MF, Baur Melnyk A (2015) Diffusion imaging of the vertebral bone marrow. NMR Biomed n/a–n/a.
41. Biffar A, Dietrich O, Sourbron S, Duerr H-R, Reiser MF, Baur Melnyk A. Diffusion and perfusion imaging of bone marrow. Eur J Radiol. 2010;76:323–8.
42. Biffar A, Schmidt GP, Sourbron S, D'Anastasi M, Dietrich O, Notohamiprodjo M, et al. Quantitative analysis of vertebral bone marrow perfusion using dynamic contrast-enhanced MRI: initial results in osteoporotic patients with acute vertebral fracture. J Magn Reson Imaging. 2011;33:676–83.
43. Schick F, Forster J, Einsele H, Weiss B, Lutz O, Claussen CD. Magnetization transfer in hemopoietic bone marrow examined by localized proton spectroscopy. Magn Reson Med. 1995;34:792–802.
44. Yoshioka H, Onaya H, Anno I, Takahashi H, Niitsu M, Itai Y. Fat tissue: relationship between chemical shift and magnetization transfer. Radiology. 1995;195:573–5.
45. Amano Y, Kumazaki T. Magnetization transfer imaging of bone marrow with and without fat suppression. Acad Radiol. 1997;4:812–5.

46. Amano Y, Kumazaki T. Correlation between water content and magnetization transfer ratio of the water component in bone marrow using gradient-echo imagings: normal case study. Skelet Radiol. 1998;27:484–7.
47. McCollough CH, Leng S, Yu L, Fletcher JG. Dual- and multi-energy CT: principles, technical approaches, and clinical applications. Radiology. 2015;276:637–53.
48. Lee S, Choi Y-N, Kim H-J. Quantitative material decomposition using spectral computed tomography with an energy-resolved photon-counting detector. Phys Med Biol. 2014;59:5457–82.
49. van Hamersvelt RW, Schilham AMR, Engelke K, den Harder AM, de Keizer B, Verhaar HJ, et al. Accuracy of bone mineral density quantification using dual-layer spectral detector CT: a phantom study. Eur Radiol. 2017;27:4351–9.
50. Mei K, Schwaiger BJ, Kopp FK, Ehn S, Gersing AS, Kirschke JS, et al. Bone mineral density measurements in vertebral specimens and phantoms using dual-layer spectral computed tomography. Sci Rep. 2017;7:17519.
51. Pache G, Krauss B, Strohm P, Saueressig U, Blanke P, Bulla S, et al. Dual-energy CT virtual noncalcium technique: detecting posttraumatic bone marrow lesions—feasibility study. Radiology. 2010;256:617–24.
52. Zbijewski W, Sisniega A, Stayman JW, Thawait G, Packard N, Yorkston J, et al. Dual-energy imaging of bone marrow edema on a dedicated multi-source cone-beam CT system for the extremities. Proc SPIE Int Soc Opt Eng. 2015;9412:94120V.
53.• Bredella MA, Daley SM, Kalra MK, Brown JK, Miller KK, Torriani M. Marrow adipose tissue quantification of the lumbar spine by using dual-energy CT and single-voxel (1)H MR spectroscopy: a feasibility study. Radiology. 2015;277:230–5. **In this study, Bredella et al. validate DECT for rapid bone marrow fat fraction quantification against MRS.**
54. Hui SK, Arentsen L, Sueblinvong T, Brown K, Bolan P, Ghebre RG, et al. A phase I feasibility study of multi-modality imaging assessing rapid expansion of marrow fat and decreased bone mineral density in cancer patients. Bone. 2015;73:90–7.
55. Arentsen L, Hansen KE, Yagi M, Takahashi Y, Shanley R, McArthur A, et al. Use of dual-energy computed tomography to measure skeletal-wide marrow composition and cancellous bone mineral density. J Bone Miner Metab. 2017;35:428–36.
56. Fletcher JW, Djulbegovic B, Soares HP, Siegel BA, Lowe VJ, Lyman GH, et al. Recommendations on the use of 18F-FDG PET in oncology. J Nucl Med. 2008;49:480–508.
57. Grant FD, Fahey FH, Packard AB, Davis RT, Alavi A, Treves ST. Skeletal PET with 18F-fluoride: applying new technology to an old tracer. J Nucl Med. 2008;49:68–78.
58. Comar D, Cartron J-C, Maziere M, Marazano C. Labelling and metabolism of methionine-methyl-¹¹C. Eur J Nucl Med. 1976;1:11–4.
59. Deloar HM, Fujiwara T, Nakamura T, Itoh M, Imai D, Miyake M, et al. Estimation of internal absorbed dose of <emphasis type="SmallCaps">l</emphasis>−[methyl-<superscript>11</superscript>C]methionine using whole-body positron emission tomography. Eur J Nucl Med. 1998;25:629–33.
60. Lee S-G, Gangangari K, Kalidindi TM, Punzalan B, Larson SM, Pillarsetty NVK. Copper-64 labeled liposomes for imaging bone marrow. Nucl Med Biol. 2016;43:781–7.
61. Paccou J, Hardouin P, Cotten A, Penel G, Cortet B. The role of bone marrow fat in skeletal health: usefulness and perspectives for clinicians. J Clin Endocrinol Metab. 2015;100:3613–21.
62. Cordes C, Baum T, Dieckmeyer M, Ruschke S, Diefenbach MN, Hauner H, et al. MR-based assessment of bone marrow fat in osteoporosis, diabetes, and obesity. Front Endocrinol. 2016;7:74.
63. Kugel H, Jung C, Schulte O, Heindel W. Age- and sex-specific differences in the 1H-spectrum of vertebral bone marrow. J Magn Reson Imaging. 2001;13:263–8.
64. Griffith JF, Yeung DKW, Ma HT, Leung JCS, Kwok TCY, Leung PC. Bone marrow fat content in the elderly: a reversal of sex difference seen in younger subjects. J Magn Reson Imaging. 2012;36:225–30.
65. Roldan-Valadez E, Piña-Jimenez C, Favila R, Rios C. Gender and age groups interactions in the quantification of bone marrow fat content in lumbar spine using 3T MR spectroscopy: a multivariate analysis of covariance (Mancova). Eur J Radiol. 2013;82:e697–702.
66. Maciel JG, de Araújo IM, Carvalho AL, Simão MN, Bastos CM, Troncon LEA, et al. Marrow fat quality differences by sex in healthy adults. 2016; https://doi.org/10.1016/j.jocd.2016.08.002.
67. Pansini V, Monnet A, Salleron J, Hardouin P, Cortet B, Cotten A. 3 tesla (1) H MR spectroscopy of hip bone marrow in a healthy population, assessment of normal fat content values and influence of age and sex. J Magn Reson Imaging. 2014;39:369–76.
68. Li X, Shet K, Xu K, Rodriguez JP, Pino AM, Kurhanewicz J, et al. Unsaturation level decreased in bone marrow fat of postmenopausal women with low bone density using high resolution magic angle spinning (HRMAS) 1 H NMR spectroscopy. Bone. 2017;105:87–92.
69. Cohen A, Shen W, Dempster DW, Zhou H, Recker RR, Lappe JM, et al. Marrow adiposity assessed on transiliac crest biopsy samples correlates with noninvasive measurement of marrow adiposity by proton magnetic resonance spectroscopy ((1)H-MRS) at the spine but not the femur. Osteoporos Int. 2015;26:2471–8.
70. Mistry SD, Woods GN, Sigurdsson S, et al. Sex hormones are negatively associated with vertebral bone marrow fat. Bone. 2017;108:20–4.
71. Salas-Ramirez M, Tran-Gia J, Kesenheimer C, Weng AM, Kosmala A, Heidemeier A, et al. Quantification of fat fraction in lumbar vertebrae: correlation with age and implications for bone marrow dosimetry in molecular radiotherapy. Phys Med Biol. 2017;63:025029. https://doi.org/10.1088/1361-6560/aa9a28.
72. Aoki T, Yamaguchi S, Kinoshita S, Hayashida Y, Korogi Y. Quantification of bone marrow fat content using iterative decomposition of water and fat with echo asymmetry and least-squares estimation (IDEAL): reproducibility, site variation and correlation with age and menopause. Br J Radiol. 2016;89:20150538.
73. Sambuceti G, Brignone M, Marini C, Massollo M, Fiz F, Morbelli S, et al. Estimating the whole bone-marrow asset in humans by a computational approach to integrated PET/CT imaging. Eur J Nucl Med Mol Imaging. 2012;39:1326–38.
74.•• Schraml C, Schmid M, Gatidis S, Schmidt H, la Fougère C, Nikolaou K, et al. Multiparametric analysis of bone marrow in cancer patients using simultaneous PET/MR imaging: correlation of fat fraction, diffusivity, metabolic activity, and anthropometric data. J Magn Reson Imaging. 2015;42:1048–56. **Schraml et al. instigate for the first time connections between bone marrow metabolic function using PET and MR imaging parameters.**
75. Patsch JM, Li X, Baum T, Yap SP, Karampinos DC, Schwartz AV, et al. Bone marrow fat composition as a novel imaging biomarker in postmenopausal women with prevalent fragility fractures. J Bone Miner Res. 2013;28:1721–8.
76. Breault SR, Heye T, Bashir MR, Dale BM, Merkle EM, Reiner CS, et al. Quantitative dynamic contrast-enhanced MRI of pelvic and lumbar bone marrow: effect of age and marrow fat content on pharmacokinetic parameter values. AJR Am J Roentgenol. 2013;200:W297–303.
77. Krings A, Rahman S, Huang S, Lu Y, Czernik PJ, Lecka-Czernik B. Bone marrow fat has brown adipose tissue characteristics, which are attenuated with aging and diabetes. Bone. 2012;50:546–52.
78. Lee P, Brychta RJ, Collins MT, Linderman J, Smith S, Herscovitch P, et al. Cold-activated brown adipose tissue is an independent predictor of higher bone mineral density in women. Osteoporos Int. 2013;24:1513–8.